Chapter 3
Research on the Characteristics and Slope Deformation Regularity of the Badong Formation in the Three Gorges Reservoir Area

Huiming Tang, Xinli Hu, Qinglu Deng, and Chengren Xiong

Abstract The Three Gorges reservoir area is characterized by widely distributed strata of the Badong formation, in which large-size landslides and deep-reaching loosely consolidated formations are likely to occur. Therefore, it is significant to reveal the mechanism and patterns of the large-size landslides that occur in the Badong formation for a better understanding of the development of the nature of deformation and process of formation of the deep-trending loose-slope stratum in the Wushan, Fengjie, and Badong renewal city zones. In this chapter, the geological characteristics of the rock mass of the Badong formation are analyzed on the basis of a systematic explanation of the rock mass strata, space variation of the lithological combinations as well as the space variation of stratum thickness, and structural deformation of the Badong formation. To demonstrate the basic law of long-term deformation of the Badong formation slopes and the patterns of later stage reformation and landslide evolution, the authors use the Huangtupo landslide as an example, as it is a typical failure in the Badong formation.

Keywords The Three Gorges Reservoir · Badong formation · Landslide · Huangtupo landslide · Landslide evolution pattern

Introduction

The Three Gorges reservoir area is characterized by widely distributed strata of the Badong formation, in which large-size landslides and deep-reaching loosely consolidated formations are likely to occur. Therefore, it is significant to analyze the mechanism and patterns of the large-size landslides in the Badong formation for a better understanding of the development of the nature of deformation and process of formation of the deep, loosely consolidated stratum in the slopes in the Wushan, Fengjie, and Badong renewal city zones. Still, profound research on the character of

H. Tang (✉)
China University of Geosciences (Wuhan), Lumo Road, Wuhan 430074, China
e-mail: tanghm@cug.edu.cn

F. Wang, T. Li (eds.), *Landslide Disaster Mitigation in Three Gorges Reservoir, China*, Environmental Science and Engineering, DOI 10.1007/978-3-642-00132-1_3,

strata construction of the Badong formation is recognized as reliable and essential geological background information in terms of reservoir bank slope protection and other types of landslide mitigation for relevant areas of the Badong formation in the Three Gorges reservoir area (Wu 1996; Zong et al. 1996).

The research on the engineering characteristics of the Badong formation in the Three Gorges reservoir area covers the following aspects: the substantial composition and engineering properties, the physical–mechanical property of the rock and soil, the hydrogeological and geological structure of the slopes, and the dynamic characteristics of ground water in the rock mass. The relation between interaction of ground water–rock mass and slope deformation and destruction, the evidence of deformation of rock masses, the configuration of loosely consolidated formations, the features of the slope deformation, and the landslide evolution patterns are also included.

In this chapter, the geological engineering characteristics of the rock mass structure of the Badong formation are based on the systematic introduction of the rock mass of strata, space variation of the lithology combinations, space variation of stratum thickness, and structural deformation of the Badong formation. To demonstrate the basic law of long-term deformation and failure of the Badong formation slopes as well as the modes of later stage deformation and landslide evolution, the authors present the example of the Huangtupo landslide, a landslide that is typical of those occurring in the Badong formation.

Development Characteristics and Space Variation of the Strata of the Badong Formation in the Three Gorge Reservoir Area

The strata of the Badong formation fall into the categories of middle Triassic System (T_2b), with the overlying strata of upper Triassic System of Xujiahe formation (T_3xj, in Wushan and Fengjie) or Shazhenxi formation (T_3s in Zigui Basin) and the underlying strata of the lower Triassic System of Jialingjiang formation (T_1j).

The Lithology and Space Variation of Lithology Combinations of the Strata of the Badong Formation

The lithology and lithological combinations of the Badong formation are subject to space variation in terms of some differences.

The 1st section of the Badong formation (T_2b^1): Wholly of grey and dark grey, the lithological combinations consist of calcareous shale, dolostone, and pelmicrite containing marlite of medium to slight lamella, all of which are brecciated to various degrees. The rock mass in this area is subject to weathering and is of low strength for soft and sub-soft lithology, with no remarkable variation in different sections.

The 2nd section of the Badong formation (T_2b^2): Wholly of fuchsia and composed of combinations of mudstone and politic siltstone, with slight variation in

various sections; in Daxi of Wushan Mountain and Fanjiaping of Badong, the crimson clastic rock mass accounts for the absolute majority except for rare grey carbonate terrain; in Guojiaba and Shazhenxi of Zigui, the crimson clastic rock mass accounts for majority except for a few grey carbonate terrain on the top of the stratum; in the Changdang of the Fengjie, the crimson clastic rock mass accounts for the majority except for a certain amount of grey carbonate terrain.

The 3rd section of the Badong formation (T_2b^3): Unchanging color of terrain in various stratum sections in terms of light grey to dark grey, the majority of rock mass is shale containing muddy carbonate rock. The content of the muddy interlayer of the terrain is characterized by an unremarkable increase from the east to the west, and the majority of the stratum falls into hard rock.

The 4th section of the Badong formation (T_2b^4): Spatially, the section of the most prominent variation of lithology in the Badong and Zigui districts in the east, where the terrain of crimson clastic rock mass accounts for the majority and is subject to a sharp decrease to the west up to the Wushan Mountain area; by contrast, the muddy carbonate terrain increases remarkably, and the grey muddy carbonate terrain increases to an equivalence of clastic terrain to Fengjie district. The majority of strata fall into soft and sub-hard rock mass.

The 5th section of the Badong formation (T_2b^5): Wholly of light grey to celandine green from the east to the west, and the lithology is subject to slight variation in terms of dolomite in the lower stratum and pelmicrite in the upper stratum in Zigui, clay rock in the lower stratum and pelmicrite in the upper stratum in Badong, as well as muddy pelmicrite in the lower stratum and clay rock in the upper stratum in Wushan Mountain and Fengjie districts.

Space Variation of Stratum Thickness of Badong Formation

Figure 3.1 is the histogram of strata measured, generally, and it is characterized by thick stratum in the east and thin stratum in the west; for instance, the total thickness of stratum in Zigui is some 830 m and that in the Changdang village of Fengjie county is about 1420 m. The 4th section has the most remarkable variation of stratum thickness in terms of 274 m in Zigui to 590 m in Fengjie.

One common outcome as shown by the predecessors' information and measurements is that the horizontal stratum thickness of the Badong formation is unstable and subject to great variation. The spatial differences of stratum thickness of the Badong formation are attributed to three factors: different thickness of deposition, uneven denudation, and impact of subsequent structural deformation.

The Badong formation represents the deposition characteristics during the transition from typical neritic mesa strata (T_1j) to continental strata (T_3xj), with general deposition in the context of shore land–tidal flat and shore land–lagoon, including inter-tide and shore land mesa strata in local sections (mainly of T_2b^3). The deposition condition is characterized by longitudinal upward shake and transverse undulating fluctuation; the former results in featured alternating occurrence of stratum of muddy carbonate rock mass and muddy stone stratum, and the latter leads to variation of deposition facies and deposition thickness.

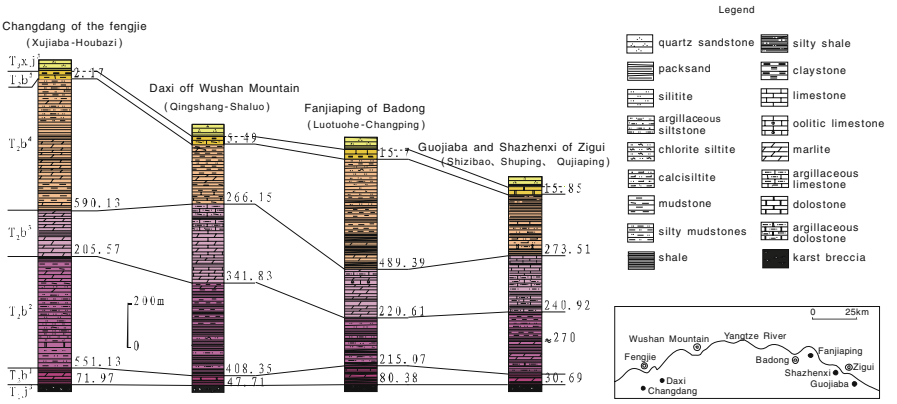

Fig. 3.1 Histogram for comparison of the strata measured in Fengjie–Wushan Mountain–Badong–Zigui of the Badong formation

The shake of longitudinal upward strata is incident to shake of raising and dropping of the crust, and local section is bare on the ground during the crust rise and subject to weathering denudation; due to the transverse undulating fluctuation of the earth surface, the ground is subject to denudation of various degrees, causing different thicknesses of residual strata.

Characteristics of Structural Deformation of Badong Formation

Cleavage

The cleavage structure of the Badong formation in the Three Gorges reservoir area is distinctive in terms of dense development and a constantly occurring strata layer, which, being weak and soft in structure, is all important in the course of the evolution of deformation and loss of stability of large-size slopes. In this section, emphasis shall be given to introducing the property of cleavage structure in the new city zone of Badong.

(1) *Attitude characteristics*: In the slope area of the Badong county, the cleavage runs in a steady manner from the old Xinling town to the new county of Xirang. Figure 3.2 is a rose diagram of the strikes drawn as per growth of 50 cleavages, and as illustrated, the predominant direction of cleavage running is evident (within the range of 80–100°), with a mean strike of 90.4° that is consistent to the extension direction of the fold axis in this area. The dip angle of the cleavage is closely related to strata lithology. The growth and the attitude of cleavage are variable corresponding to different positions of the fold and various lithology sections. The cleavage is nearly vertical at the fold core, which is generally in the opposite direction to the layers in the wing sides. Same-direction cleavage is only found in the 2nd section of the Badong formation, and the cleavage is featured by steep dip angle. In general,

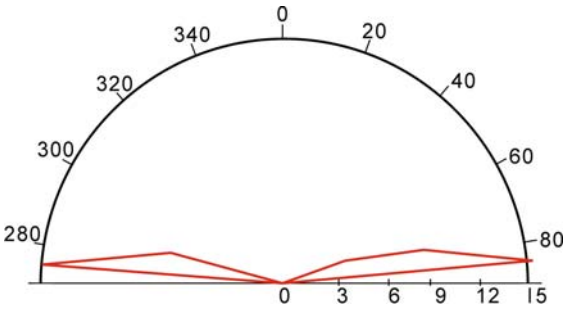

Fig. 3.2 Rose diagram of cleavage strike in Badong county

the angle between cleavage and stratum is great (72–90°) in the 3rd section of the Badong formation; that is less (36–60°) in the 2nd section of the Badong formation, an outcome of mud content of the rock mass in terms of higher content of mud and less angle.

(2) *Extent and pattern of cleavage development and relations between cleavage and stratum lithology*: The different stratum lithology has a remarkably diversified extent of cleavage development. For example, cleavage is hard to find in the Jialingjiang formation, but by contrast, the cleavages develop well in the 2nd and the 4th sections of the Badong formation in terms of the cleavage spacing generally of millimeter to centimeter levels; the cleavage is dense in the 3rd section in terms of cleavage spacing of centimeter to tens of centimeter levels as well as thinner stratum develops better than that of thicker one and stratum of higher content of mud develops better than that of lower content of mud; as for the 3rd section, the upper stratum develops better than the lower stratum. In addition, different position of one stratum has different type of cleavage. The cleavage of the 3rd section is typically noncontinuous in terms of separate interface between the cleavage composed of muddy (or sericite) membrane and muddy pelmicrite split rock; and the 2nd and the 4th sections are characterized by continuous cleavages, where the cleavage domain and split rock are hard to differentiate in the open except for visible flake-shape exfoliation along the length of cleavage which extends in the mantle rock.

(3) *Cleavage structure*: Emphasis is given to outdoor and indoor observations and research of the 3rd section, and the result shows gradual and fluctuating development of cleavage instead of a straight and flat face (Fig. 3.3), and the cleavage domain looks like a narrow and long lens. The thickness of the cleavage domain of a dark celadon muddy stratum ranges from nearly 1 to 5 mm; for more careful observation, this stratum is differentiable to several strata (muddy) of less thickness, sandwiched by thin layer of white and fine crystal calcite in the form of a multilayer pie. To observe this stratum under a microscope, the multilayer structure is clear, among which the muddy pelmicrite observed in the open is fine sericite flakes arrayed in a given direction, and the fine crystal calcite stratum develops vertical to the rock wall, with joints vaguely visible at the center (Fig. 3.4).

Fig. 3.3 Cleavage of muddy pelmicrite of the 3rd section of Badong formation

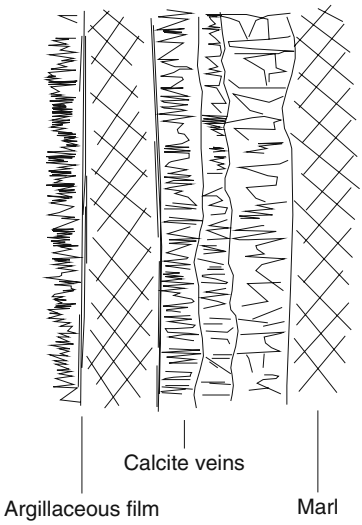

Fig. 3.4 Sketch of microscopic cleavage structure

Joint

The joint develops well in the Badong county area, where the pattern of the valley is subject to impact by the joint. The joints in this area can be divided into four groups according to directions, namely, EW, SN, NNE, and NNW.

(1) *EW joint*: It belongs to a longitudinal joint, mainly found in the broad and smooth section from the Guandukou in the riverfront to the core of the syncline, where the joint is flat and straight and unfilled in most of the area as well as of moderate to smooth obliquity. This is a conjugate joint of *s* parallel intersecting line (east–west)

that is probably formed as a result of pressing stress field in adjacent to south–north direction.

(2) *SN joint*: It belongs to transverse joint and falls into shear joints and tension joints as per mechanical quality. The shear joint is steep, level, regular and extends afar (generally of tens to hundreds of meters), and the joint is isometric in transverse direction (normally with spacing of 500–600 m), and this joint group has impact on the valley of Badong county area. The tension joint develops mainly in hard rock mass with a steep joint face, and the face is irregular, nonlinear and generally extends to within tens of meters; most of the tension joints are of the branch end, with the gap filled by calcite range. According to statistics of more than 40 tension joints in the Sidaogou Valley, the mean strike of the joint is 5°, and the predominant direction is concentrated and nearly vertical to the cleavage side. In comparison to the shear joint of the same direction, it extends in shorter distance and is denser in terms of varied spacing within the range of 0.2–7 m.

(3) *NNE and NNW joints*: Both of them are generally in the pattern of conjugate joints and can be found in different lithological sections. Generally, the joints are dense and extend a short distance within the range of several centimeters to less than 20 m. Thus, the direction of main pressure stress in conjugate joints is northeast.

The conjugate joints, SN tension joint and EW joint reflect the stress field of the same structure, i.e., are the main stress adjacent to south–north direction. The SN shear joint probably falls into the group of conjugate joints in terms of direction, but both are hard to match in modeling.

Geological and Construction Property of the Rock Mass Structure in the Badong Formation

Property of Rock Mass Structure

Research on properties of the rock mass structure is accomplished mainly by means of statistics about structural planes and Monte Carlo simulation. Due to many stages of crust movement and impact of the Yangtze River cutting and eroding, the structure joint and unloading fissures of the rock mass of the Badong formation are well developed. The structure of the rock mass is composed only of these structural planes and rock blocks. Therefore, the dimension of structure mass and geometric property of the structure can be determined by means of an analog of combination characteristics, distribution and extension patterns, and the development condition of the structure planes, which is an effective method for studying the structural property of a rock mass.

The bedrock of an example outcrop in Badong county is selected as the section for surveying and statistics, and each of the geometric pattern parameters of each structural plane is measured using the linear statistical method, with nine measuring lines arranged in succession.

The principles of a Monte Carlo network analog are employed to draw the network diagram and networking diagram of bedrock structure planes within the area so as to determine the distribution chart of line density and RQD value of various directions of the section.

The following conclusions can be made through applying statistics of structure planes and network analogs of structure planes of rock mass:

(1) The research shows general development of 3–4 joint groups in the rock mass in this area, and the joints are characterized by steep slope angle (generally of 45–80°) in the directions of adjoining east, NNE, and near west.
(2) The variation of the attitude of the strata is remarkable and uneven, and the interlayer cleavage and secondary fold are well developed due to impact of the structure movement.
(3) Most of the joints are through structure planes, and the trace length measured is tens of meters and intersects with many groups of structural planes. By comparison, the trace length of other structure planes is less, with half the trace length of 1.0–5.0 m and a few of more than 5.0 m; according to the information collected by surveying and statistics, the width of most fissures between structure planes is less than 5 mm and within the range of 1–3 mm, and the fissures are rarely filled and are open. The joints in the muddy rock mass are short and small.
(4) The structural planes have large mean spacing, and remarkable differences exist between different groups of structure plane, generally of 30–300 cm, a minimum of 3 cm and a maximum of 650 cm. In general, the linear density of structure plane is 1.5–4.0 lines/m, some 0.24 lines/m in the least dense area and some 8.34 lines/m in the densest area, with directions of the most concentrated in 5–25°, 55–70°, 130–165° as well as directions of the most densest lines in 15–40°, 85–100°, and 115–170°.
(5) In this area, the RQD value is tremendous at the block diameter of 0.1 m, with mean RQD at various surveying points of more than 90%; and the RQD is less at the block diameter of 0.5–0.7 m, with remarkable differences between various surveying points; most of the values are more than 60%, showing that the rock mass is large in this area. The structure of the rock mass is featured by layered pattern or layered fracture patterns.

Physical–Mechanical Property of the Soft Layer

The physical–mechanical property of the soft layer is very much dependent upon the slope stability. As shown in Table 3.1, the landslide soil, muddy sandwich, and fault mud in the terrain weak zone are of fine granularity and fall into silty clay and have low values of shear strength (slow shear stress) C and ϕ.

Table 3.1 Analysis of physical–mechanical properties of the terrain weak zone and landslide zone of the Badong formation

Sample No.	Moisture content	Unit weight	Granule composition					Cohesion	Internal friction angle	Classification according to composition
	W	*r*	0.25–0.1	0.1–0.05	0.05–0.01	0.01–0.005	0.005–0.002	*C*	ϕ	
	%	g/cm^3	%	%	%	%	%	kPa	°	
1#	18.4	1.95	4.7	2.0	15.0	32.4	45.9	20/10	11.3/14	Light silty clay
2#	30.4	1.74	4.6	7.0	23.7	23.8	40.9	88/72	32/31	Light silty clay
3#	11.1	1.95	5.1	3.4	47.3	22.0	22.2	70/60	32/33.7	Light silty clay
4#	37.2	1.45	4.3	3.1	14.8	30.4	47.4	5.0/5.0	12.5/10.3	Light silty clay
5#	16.6	1.69	0.5	4.3	30.8	18.0	46.4	10.0/5.0	19.2/18.4	Light silty clay
6#	11.4	1.89	23.6	8.6	22.6	12.3	32.9	5.0/5.0	19.9/19.7	Light silty clay

Engineering Properties of the Rock Mass

Physical–Mechanical Property of the Rock Mass

The basic physical–mechanical property of the rock of the Badong formation includes: (1) T_2b^2 and T_2b^4 muddy siltstone, the muddy rock is generally of soft rock and sub-soft rock, and most of T_2b^3 are of high strength, with saturated tension strength of more than 30 MPa, fall into sub-hard or extremely hard rock, and physical–mechanical property of T_2b^1 is between the two types of rock as mentioned above; (2) The mechanical strength is subject to impact of structure planes and density, for instance, the mechanical strength and density (minimum of ρ_d=2.3 g/cm^3) of thin marlite and calcareous muddy siltstone are the least, and their spacing rate is the highest (n is up to 1.93–4.72%); (3) The muddy rock varieties are subject to high intenerating, and the softening coefficient of most of the muddy rocks is less than 0.6; by contrast, the pelmicrite varieties are subject to weak intenerating and have softening coefficient of more than 0.75, showing greater impact of muddy rocks (e.g., silty rock, calcareous muddy siltstone, and muddy pelmicrite) to mechanical property; (4) According to the point load test, various types of rock have strong anisotropy, and the rock strength is estimated by the point load strength and the uniaxial strength of rock mass.

Mechanical Properties of the Structural Plane

(1) *Indoor shear test*: The test of the structural plane shows that the shearing strength of the terrain and that of the cleavage is approximately equivalent with identical lithology, and the shearing strength is slightly different with strata of various lithology; for instance, the T_2b^1 is thin marlite and subject to severe weathering, covered with muddy membrane on the surface, and its strength is comparatively lower than that of other groups of rock; C is generally of 5–15 kPa, ϕ is 20–30°, as to T_2b^3pelmicrite, C is 50–100 kPa and ϕ is 30–38°.

(2) *Inverse calculation of cuneiform body and statistics of the bedrock landslide*: According to research and statistics for the landslide of cuneiform body and bedrock of various types of rocks, the shearing strengths C and ϕ of various structure planes are calculated. A total occurrence of five cuneiform bodies are found mainly in the case of T_2b^2 fuchsia, a calcareous muddy siltstone; the sliding plane is composed of a layer and nearly vertical intersecting cleavage plane in all cases. The dimension of the cuneiform body is measured on the spot, and the stability coefficient formula of cuneiform body is applied. The shear strength of the landslide planes (layer and cleavage plane) can be worked out through a random choice of 4 of 5 landslides. Also, the calculated coefficient of shear strength of layers and that of cleavage plane of T_2b^2fuchsia calcareous muddy siltstone is approximately equivalent of $C_{layer}=C_{cleavage}$=6.8–12.8 kPa, $\overline{C}$=8.6 kPa; $\phi_{layer}=\phi_{cleavage}$=26–39.5°, $\overline{\phi}$=35°. The result is slightly less than the value (T_2b^2 layer C=110 kPa, ϕ=38°) of indoor shear test of the structure plane. According to research, the occurrences of landslide of cuneiform body in this area occur in the rainstorm season, when the strength of the

sliding plane is lowered due to rainwater saturation and lubrication, etc.; indoor tests are completed in dry conditions, hence the outcome of inverse algorithm is less than the test data.

Bedrock landslides occur mainly in strata of T_2b^3 and T_1j; in some sections and due to artificial excavation of the slope, the bedrock is bare, and the rock mass loses support, causing a bedrock landslide. This occurrence is similar to a single plane landslide of slope failure, when the slope angle of the sliding plane is approximately equivalent to its friction angle in the condition of limit balance. The approximate friction angle can be calculated through surveying a great amount of slope angles of various sliding planes. The mean friction angle of T_2b^3 pelmicrite $\overline{\phi} = 38^\circ$, basically equivalent to that obtained in indoor shearing tests of the structure plane.

Estimation of Mechanical Parameters of Rock Masses

(1) *Evaluation of rock mass quality*: According to the engineering and geological property of rock masses, the rock mass is divided into four groups, and then evaluations of qualities of various rock groups are applied by means of classification of RMR and Q value (Table 3.2). The results of classification demonstrate that the rock mass qualities estimated with both methods of classification are basically equivalent.

(2) *Calculation of mechanical parameters of rock masses*: The deformation modulus E_m (Gpa) of various types of rock mass can be calculated by means of the RMR and Q values, as shown in Table 3.3. According to the RMR value of various types of rock mass, corresponding C_m and ϕ_m values can be looked up (Table 3.4). The mechanical parameters of various types of rock mass can be worked out by the Hock–Brown estimation method (Table 3.5).

Table 3.2 Classification of rock masses

Item	I	II	III	IV
Stratum lithology	T_2b^2, T_2b^4 siltstone and muddy siltstone	T_2b^3 pelmicrite	T_2b^3 marlite	T_2b^3, T_2b^1 pelmicrite and shale
Q classification	3.29	11.5	3.83	1.01
RMR classification	52	66	54	32
Rock type	Common quality	Good quality	Common quality	Poor quality

Table 3.3 Estimation of deformation modulus of rock masses

	I	II	III	IV
RMR value	52	66	54	32
E_m (GPa)	11.2	32	12.5	3.5
Q value	3.29	11.5	3.83	1.01
E_m (GPa)	12.9	26.5	14.5	0.11

Table 3.4 Strength parameters of rock masses calculated by the RMR classification method

		I	II	III	IV
RMR value		52	66	54	32
Shear strength	C_m(kPa)	260	325	270	150
	ϕ_m (°)	31	38.0	32	22

Table 3.5 Estimation of mechanical parameters of rock masses by the Hock–Brown method

Rock group	Uniaxial stress strength σ_c (MPa)	Uniaxial stress strength σ_{mc} (MPa)	Uniaxial tension strength of rock mass σ_{mt} (MPa)	Parameters of shear strength of rock masses in different positive stresses	
				Cohesion (Mpa)	Friction angle (°)
				0 2 4 6 15	0 2 4 6 15
I	30	1.12	0.05	0.12 0.47 0.76 0.95 1.86	57 26 21 19 14
II	75	3.18	0.16	0.37 0.81 1.15 1.47 2.64	58 34 29 26 20
III	100	6.32	0.6	1.20 1.59 2.00 2.38 3.65	53 39 34 31 25
IV	20	0.2	0.01	0.03 0.34 0.51 0.69 1.21	61 18 15 13 10

Recommended Parametric Values for Mechanical Calculation of Rock Mass

In integrating various existing data as well as data concerning mechanical property and experience of identical rock mass in relevant adjoining areas and in consideration of factors such as geological and structural properties, etc., of various rock masses in the areas, we recommend the following parametric values for calculation of various rock masses and structure planes, as shown in Tables 3.6 and 3.7

Table 3.6 Recommended parametric values for mechanical calculation of rock masses

	T_2b^4	T_2b^3	T_2b^2	T_2b^1	T_1j^3	T_1j^2	T_1j^1
Density ρ(g/cm^3)	2.55	2.63	2.55	2.35	2.68	2.68	2.66
Deformation modulus E_m(GPa)	2.0	4.0	3.0	1.5	10.0	9.0	7.0
Poisson′s ratio μ	0.3	0.25	0.3	0.35	0.2	0.2	0.25
Uniaxial stress strength σ_{mc} (MPa)	0.8	2.5	1.0	0.15	5.0	4.5	4.0
Uniaxial tension strength σ_{mt} (MPa)	0.03	0.50	0.05	0.01	0.5	0.45	0.4
Shear strength C_m (kPa)	240	400	260	165	1100	1100	1000
ϕ_m (°)	28	38	30	22	41	41	39

Table 3.7 Recommended parametric values for calculation of structure planes

Type of structure plane	Shear strength	
	C_j(kPa)	ϕ(°)
T_2b^3 mudstone layer	60	31
T_2b^3 mudstone cleavage plane	40	30
T_2b^2 calcareous muddy siltstone plane	20	31
T_2b^2 calcareous muddy siltstone plane cleavage plane	8	30
T_2b^1 marlite plane	8	25
T_1j pelmicrite plane	30	32

Typical Landslide of the Badong Formation – Deformation Mode of the Huangtupo Landslide

The Huangtupo landslide is located about 1 km upstream of the old Badong county of Hubei province, on the south bank of the Yangtze River, to the west of Erdaogou, and to the east of Sidaogou. In comparison to the adjoining areas, the Huangtupo is generally smooth in landform with two broad platforms. On one platform is the 1st Senior High School of Badong county and that of Badong Farm Machine factory; quaternary deposition almost accounts for the whole Huangtupo landslide, and beyond it, the bedrock predominates and the quaternary rock mass is sparsely distributed.

Geological Background

The main outcrop of the Huangtupo landslide and adjoining areas is muddy pelmicrite of the 3rd section of the Badong formation, and the outcrop behind the slope belongs to fuchsia marlite and muddy siltstone of the 2nd section of the Badong formation.

The Guandukou syncline is a main structure of this area (Fig. 3.5); the axial trace is adjacent to the east–west direction, a broad fold zone gradually widens, with an SN width of up to 6 km. The slope angles of both flanks are generally of 20–45° (Fig. 3.6). The Huangtupo landslide is in the south wing of the syncline of the dip slope.

The bedrock landslide muddy zone of the Badong formation in the new city zone is well developed. The area accelerating the initiation of the bedrock landslide

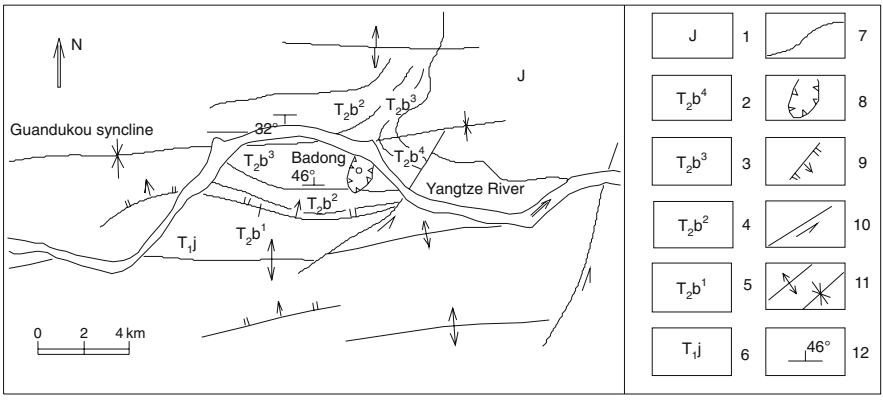

Fig. 3.5 Outline of the structure of Badong new city zone and adjoining areas. 1 – Jurassic System; 2 – the 4th section of the Badong formation; 3 – the 3rd section of the Badong formation; 4 – the 2nd section of the Badong formation; 5 – the 1st section of the Badong formation; 6 – Jialing River formation; 7 – sideline of lithology sections; 8 – landslide; 9 – normal fault; 10 – strike slip fault; 11 – fold (the left is anticline, and the right is syncline); 12 – terrain attitude

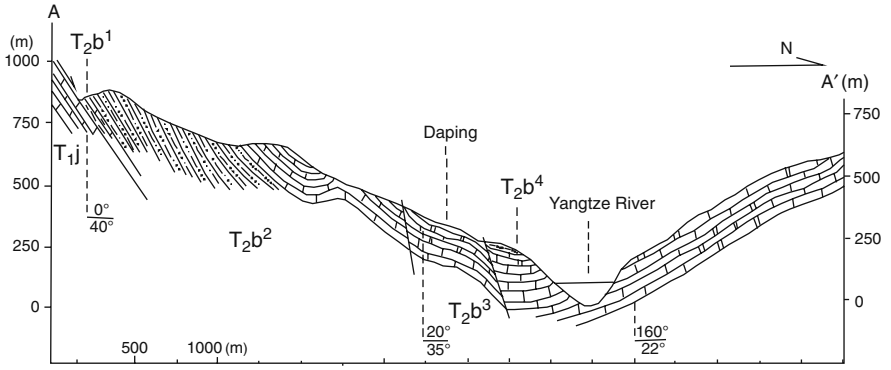

Fig. 3.6 Profile of Guandukou syncline

is where the interface of strong and weak terrains as well as a weak sandwich of the internal terrain locates, among which the former includes the interface between Jialing River stratum and the Badong formation as well as that between the 2nd and the 3rd sections of the Badong formation. The development of a fault of the Badong formation may be attributed to this bedrock landslide; and the latter develops mainly in the 3rd section of the Badong formation.

Figure 3.7 is a section of the Xirangpo Water Diversion Tunnel, where the terrain is formed by the 3rd section of the Badong formation, with length of the section plane of 210 m, wherein 14 bedding faults of various sizes are formed, and an average of one fault every 15 m develops, which is evidently, a dense development of faults; the landslide zones are of different thickness, with majority of the centimeter level and minority of more than 1 m.

The bedrock landslide zone is characterized by a muddy area, breccias muddy areas or breccias areas of low mechanical strength. Four sliding muddy areas in the tunnel are sampled for stress strength test, and the mean shearing strength obtained is C=13.3 kPa, ϕ=4°.

The dip slope, bedrock landslide area, and cleavage contribute substantially to structural deformation during generation and development of the Huangtupo landslide.

Long-Term Deformation of the Slope

According to investigations of the deformation zones on both sides of Huangtupo landslide and the front edge of the riverfront, long-term slope deformation is found in terms of coincidence of toppling deformation and deep creep deformation (Fu & Cai 1996; Carey 1953; Savage & Varnes 1987; Zischinsky 1966).

(1) *Toppling deformation*: The loosely consolidated body of the Huangtupo landslide slopes eastward, and there is a wide area of rock mass of strong deformation,

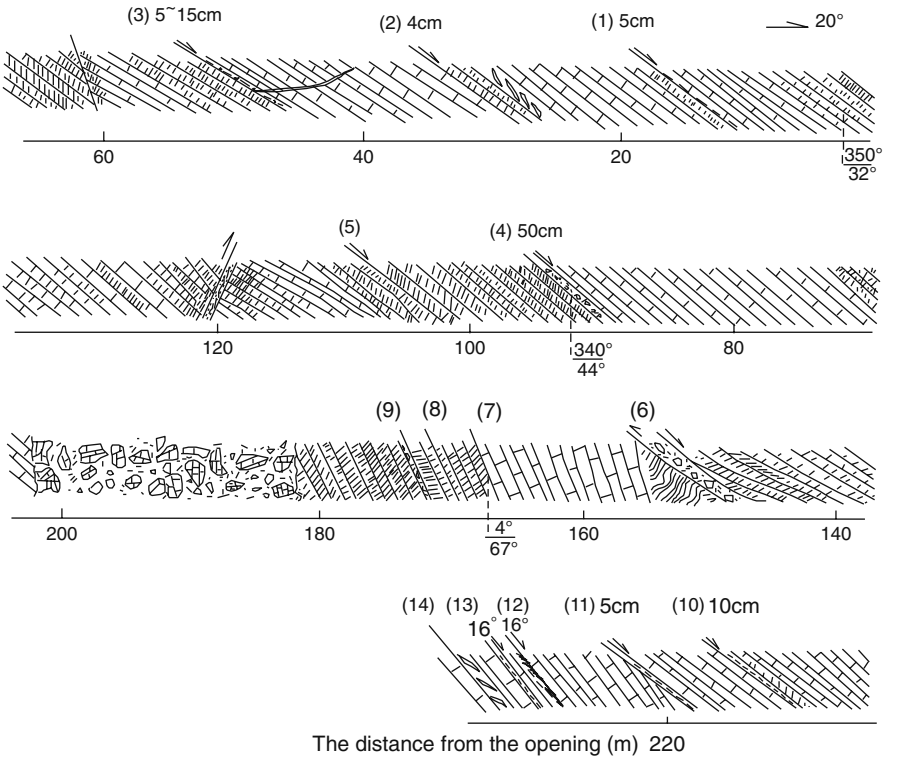

Fig. 3.7 Measured section of the water diversion tunnel on Xirang slope

characterized by toppling of rapidly developing axial cleavage (Fig. 3.8). The toppling deformation causes joint rock blocks to form in a staggered, rotating, and consequently toppling downgrade.

Although the terrain experiences strong toppling deformation, the terrain plane remains intact, and the toppled rock mass and the underlying non-toppled rock mass

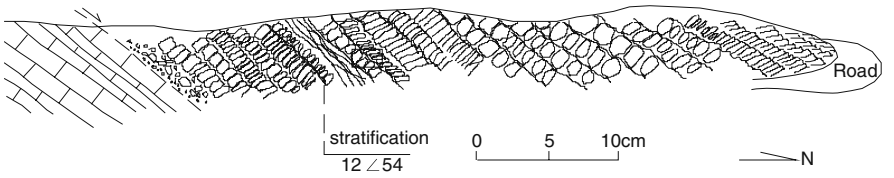

Fig. 3.8 Toppling deformation of cleavage in the east side of Huangtupo landslide

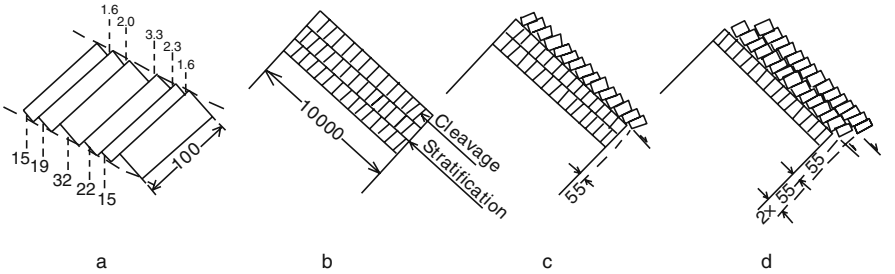

Fig. 3.9 Measurement and modeling of toppling and displacement of cleavage rock of the Emigration Bureau highway slope. a – Measurement of toppling of cleavage rock; the upper figure stands for staggering distance between cleavage rocks, and the lower figure stands for thickness of cleavage rock, in centimeter; b – cleaved single rock mass; c – toppling of cleavage of single rock mass; d – general effect of toppling of cleavage of multilayer rock mass

are separated by the sandwiched bedrock landsliding plane, and it is obvious that slippage of any long distance does not occur.

According to the rotation and staggering (Fig. 3.9a) of cleavage rock of the single terrain observed in this section, the sliding displacement of 0.55 m of the single terrain (assumed of 1.0 m of terrain thickness) of 100 m long in the front end caused by rock toppling can be estimated. Assuming that a terrain section with a thickness of 100 m (assumed of 1.0 m of terrain thickness, see Fig. 3.9b), the top terrain topples first and leads to displacement of 0.55 m in the front of the terrain (Fig. 3.9c); and then another terrain topples (Fig. 3.9d), also with displacement of 0.55 m in the front, when the front end of the upper terrain has a relative displacement of $2\times0.55 = 1.1$ m as per its original position $2\times0.55 = 1.1$ m; likewise, in the case of toppling of the 100 underlying terrains, the upper terrain has a relative displacement of $100\times0.55 = 55$ m.

In the case where the toppled rock masses fail to open along the joint, it causes longitudinal extension of the terrain, which is the cause of bedrock deformation before toppled and deformed terrains; longitudinal sliding is necessary for toppling in terms of space adjustment, and this is why there is often occurrences of displacement of development of toppled rock mass to the dip slope.

The toppled and reconstructed terrain at this observation point remains completely intact stratum; nevertheless, the toppled rock mass observed from the west side of the Huangtupo landslide is a transition of continual and intact stratum to disarrayed rock blocks from inside to outside (Fig. 3.10), and the farthest outer stratum of disarrayed rock blocks of the toppled rock mass is in identical pattern of rock deposition as formed by the landslide.

(2) *Deep creep deformation*: The front edge of the Huangtupo landslide (previously on the riverfront) is adjacent to the core of the Guandukou syncline; and the terrain is of smooth slope and simple structure, thru observing from the river in the west of Huangtupo. The structure of terrain within the Huangtupo landslide area is complicated, for instance, a reverse or knee-type asymmetric fold is found here and there

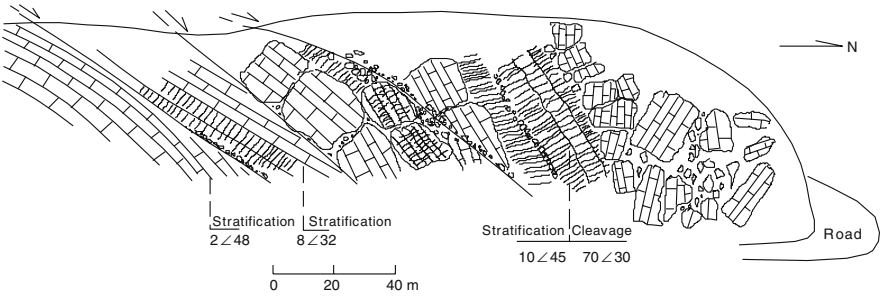

Fig. 3.10 Toppling deformation in the west side of the Huangtupo landslide

(Fig. 3.11), and the fold hinge is near the east–west direction, with axial plane facing the Yangtze River. In addition, smooth shearing slippage is common (Fig. 3.12). The direction of shearing slippage in the upper part is westward.

The deep gully (Sandaogou) of the inner Huangtupo landslide is found to be of loose surface stratum in many places, revealing the deformed rock mass in the deep area. Figure 3.13 shows one of the sections of Sandaogou, T_2b^2 formed fuchsia rock blocks deposit onto T_2b^3 muddy pelmicrite,one reverse fold with intact pattern develops under the interface, and it represents the kinematic property of the upper layer downward along the slope. Fissures develop in the fold, a universal characteristics of fold with a slope of creep deformation. The cleavage still runs in an

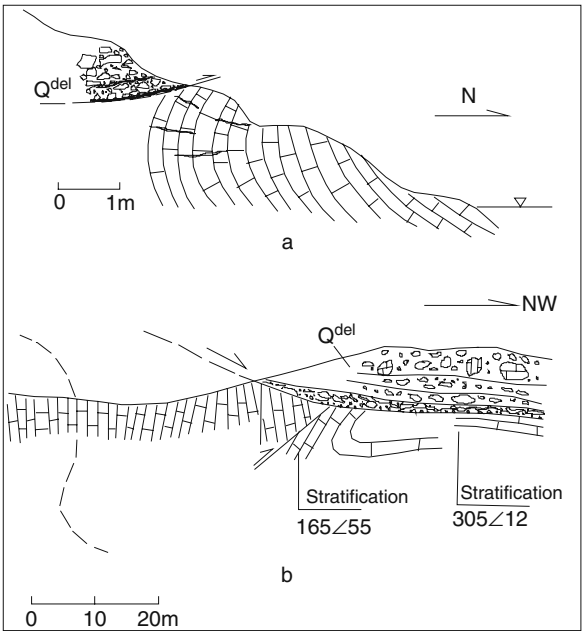

Fig. 3.11 Occurrences of slippage and fold in the front edge of the Huangtupo landslide

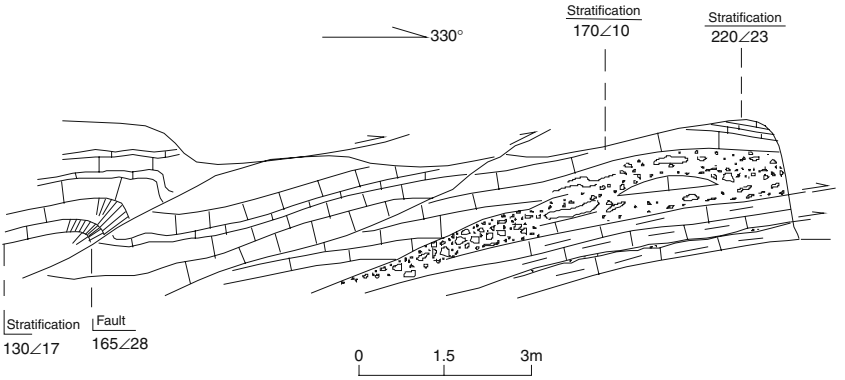

Fig. 3.12 Occurrences of asymmetric fold and shear slippage in the front edge (previously the riverfront) of the Huangtupo landslide

east–west direction, consistent to that of local cleavage, indicating that the fold rock is still part of the bedrock.

According to the fold and shearing slippage as well as the reflected kinematics property, the following characteristics can be concluded: (1) Distribution only in the front edge of the Huangtupo landslide and of loosely consolidated deposition underneath; (2) Small-size fold in terms of outcrop dimension, and the axial plane inclines downward the dip slope, just opposite to the secondary fold, produced coincidently with the longitudinal fold structure in early Guandukou; (3) The terrain fold is an outcome of creep deformation due to long-term gravity effects on the slope rock, which is inconformity to rock blocks produced by rapid deformation

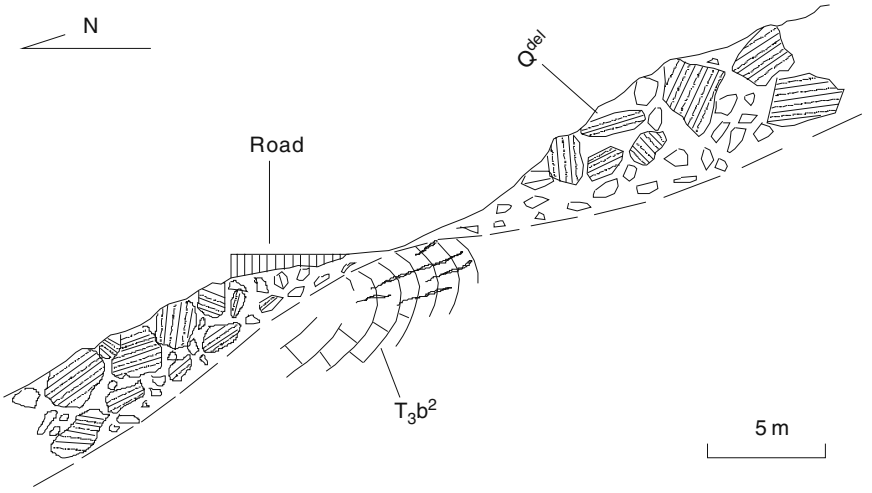

Fig. 3.13 Asymmetric fold and shearing slippage of Sandaogou of the Huangtupo landslide

of the landslide; fold turn generally goes with fissure development, which is different from the fold generated by structural stress action; (4) The movement direction of the upper area of shearing sliding plane faces the dip slope, still opposite to the bedrock landslide caused by the Guangdukou longitudinal fold structure. These characteristics demonstrate that the folds are neither the cause of formation nor the outcome of landsliding; rather, they are results of long-term creep deformation due to gravity. It can be concluded as per the deformation property of the Huangtupo landslide that the deformation is not the cause of formation of local stratum due to limits within Huangtupo domain, and that the deformation is not the outcome of landsliding because of the gradual transition relation of the deformed section and the bedrock. Also the deformation is an outcome of long-term gravity action on the slope.

Landslide

The top stratum of the Huangtupo landslide is composed of fuchsia stone blocks (T_2b^2) of the 2nd section of the Badong formation, merging onto the 3rd section (T_2b^3), with the interfacing pattern distributing in the form of insole in some NE20° as well as longitudinal length of 1100 m and width of 400–500 Mc (Fig. 3.14). The border in the front edge of T_2b^2 fuchsia stone blocks runs some 800 m to the north more than that of stratum border of T_2b^3/T_2b^2; it is obvious that this is the cause of the deposition of the landslide due to the "over-coverage" of such a large area and long distance.

(1) *Pattern of physiognomy of the Huangtupo landslide*: Two levels of platforms develop within Huangtupo. The 1st one has an elevation of 285–310 m, upon which the 1st Badong Senior High School is located, trending EW, 350 m in length and more than 100 m in width, trending SN. The 2nd platform has an elevation of 430–455 m, the Badong Substation and Badong Bus Transportation Co., Ltd are located on top of this platform, and it trends EW with a length of 370 m and an SN-trending width of 150 m. A reverse landform appears in the local section of this platform. The pattern of physiognomy of the platform is sharply in contrast to the straight slope on both sides (EW) of the Huangtupo landslide and difficult to compare with the elevation of the jump stratum, which is probably formed as a result of the landslide; due to variation of slope angle of the landslide's underside, the landslide reflects a corresponding transformation of ground pattern. The elevation is some 600 m in the rear edge of the landslide, with a dimly distinguishable pattern of sliding wall, which is generally an east–west arc physiognomy.

The slope angle is 40–45°, consistent to that of the terrain of fuchsia muddy siltstone of the 2nd section of the Badong formation (T_2b^2). This pattern of physiognomy is not limited to landslides of small size.

(2) *Section structure of the Huangtupo landslide*: The electrical method mapping is completed for the front edge of the Huangtupo landslide by the Badong formation research team from China University of Geosciences in 1997. A better

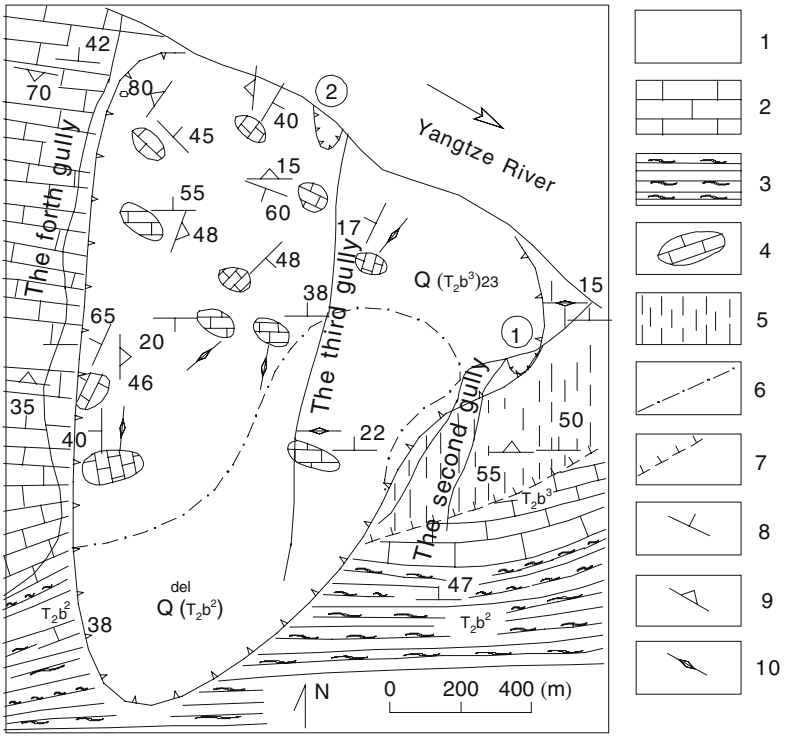

Fig. 3.14 Geological map of the Huangtupo landslide. 1 – The muddy pelmicrite of the 3rd section of the Badong formation; 2 – the muddy siltstone and silty mudstone of the 2nd section of the Badong formation; 3 – the outcrop of loose deposition of stone block (the terrain pattern and cleavage pattern marked alongside); 4 – toppling deformation area; 5 – landslide border; 6 – front border of small size landslide of Huangtupo; 7 – transition border of toppling and bedrock; 8 – terrain pattern; 9 – cleavage attitude; 10 – perpendicular cleavage; Circle 1: Erdaogou landslide; Circle 2: landslide on the west side of Sandaogou

understanding of the geological structure of the front section of the Huangtupo landslide is obtained by the analysis of resistance ratio section. Figure 3.15 (above) shows resistance ratio section of the Huangtupo landslide, and the ratio is obtained thru certain processing of resistance, reflecting the relative value of resistance and eliminating error caused by landform; Fig. 3.15 shows geological explanation as per the resistance ratio section.

(3) *Characteristics of landslide zone development*: Based on observations along the river, the front edge of the Huangtupo landslide and the landslide shear zone between the Erdaogou and Sidaogou are dimly distinguishable, and the following is description of characteristics obtained from two observation points:

Observation point 1: The riverfront 300 m in the east of Sidaogou has an elevation of some 80 m, where a breccia zone with a thickness of 2–3 m develops. The size of the breccias is mixed, ranging from 50 cm to 1–20 cm in terms of size of granules.

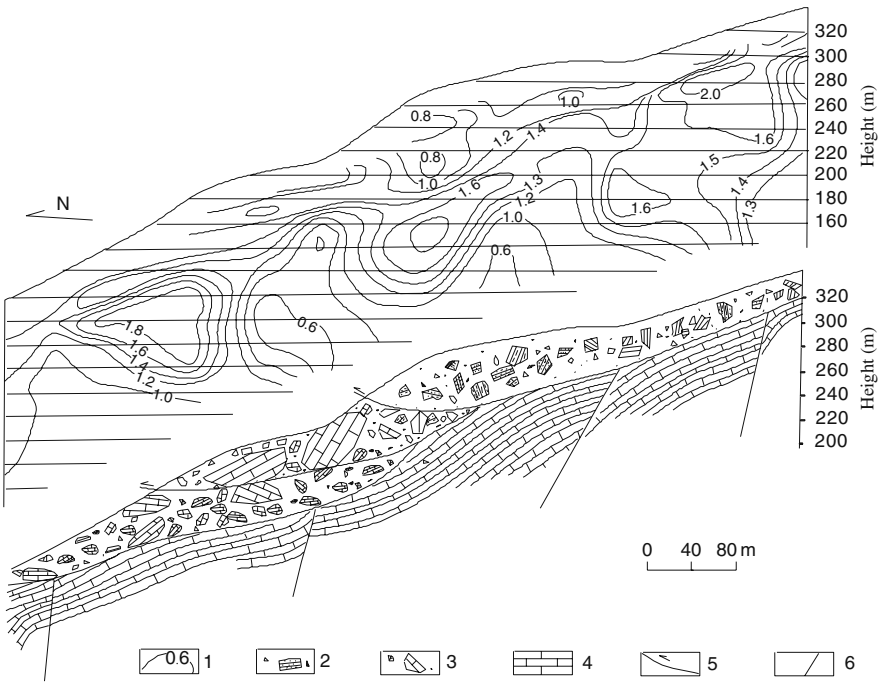

Fig. 3.15 Resistance ratio section (*above*) and geological explanation (*below*) of the Huangtupo landslide. 1 – ratio contour; 2 – stone blocks composed by muddy siltstone and silty mudstone of the 2nd section of the Badong formation; 3 – stone blocks of muddy pelmicrite of the 3rd section of the Badong formation; 4 – pelmicrite; 5 – sliding plane; 6 – fault

The breccias are subject to strong pressure, with individual ones in the form of shredded cabbage as a result of strong pressure and friction as well as released stress, which rebounds and causes surface peeling. The breccias are in the form of calcareous half cementation. The pattern of the breccias zone is 168°∠36°, with the underlying terrain reverses; as per the conclusion of the pattern variation, the upper terrain of breccias zone slides horizontally northward (Figs. 3.16a and 3.17).

Observation point 2: The breccias zone 200 m to the west of Erdaogou has a thickness of 1–1.5 m, smoothly inclines northwest (305°∠12°) and is composed of light yellow grey muddy gravel primarily in the form of roundness with manor edges and corners, as well as polished and scraped on the surface (Figs. 3.18, 3.19 and 3.20). The breccias are of various sizes and generally of several centimeters, and the percentage of breccias and mud is 25–65%. The top stratum of breccias zone is composed of fracture rock mass and cracked rock mass, and the cleavage pattern (220°∠22°) is inconsistent with the direction of local cleavage. The bottom stratum is T_2b^3 stratum subject to strong deformation, and reverse fold and pressing fault (Fig. 3.16b), etc., develop. This zone of strong deformation is an outcome of primary creep deformation.

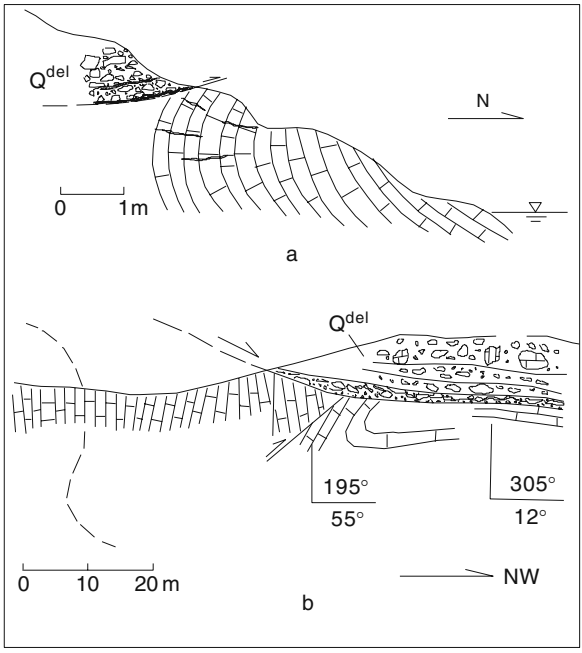

Fig. 3.16 Section of shearing outlet of the Huangtupo landslide. a – 300 m to the east of Sidaogou; b – 200 m to the west of Erdaogou

It is demonstrated from various angles that the Huangtupo landslide experiences sliding on the basis of primary creep deformation, including the front edge of the landslide. The rock mass in the Huangtupo landslide is fragmented; although rock masses of large size remained, displacement, staggering, and rotation occurred together, causing discontinuity of patterns of structure planes and lines among rock masses.

Fig. 3.17 Breccias at the shearing outlet in the front edge of the Huangtupo landslide, a shredded cabbage pattern occurs as a result of strong pressure, in the riverfront, 300 m to the east of Sidaogou

Fig. 3.18 Landslide zone in the front flank of the Huangtupo landslide, in the riverfront, 200 m to the west of Erdaogou

Observation point 3: TP3 adit reveals the sliding plane and shows clearly the contact relation between the sliding body and the sliding bedding, as well as the basic property of the sliding zone (Fig. 3.21).

The breccias or muddy breccias zone of large size in the front edge of the Huangtupo landslide (riverfront) is compatible to the loose deposition zone, certainly the outcome of the shearing outlet. Nevertheless, Huangtupo landslide is not formed overnight; instead, it is an outcome of multiple stages, characterized by loss of stability.

Fig. 3.19 Rounding and polish of breccias in the front flank landslide of the Huangtupo landslide, on the riverfront, 200 m to the west of Erdaogou

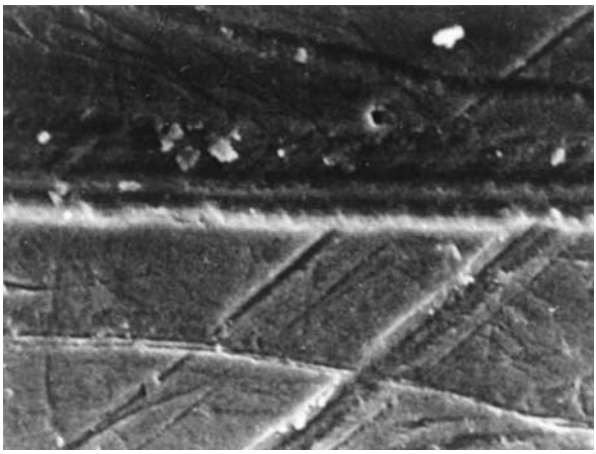

Fig. 3.20 Surface scraping of breccias in the front flank landslide of the Huangtupo landslide, on the riverfront, 200 m to the west of Erdaogou

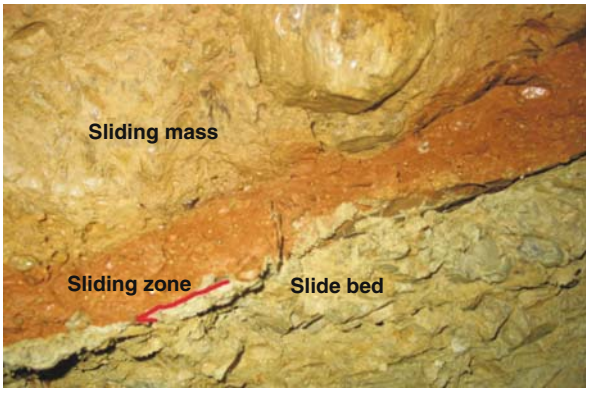

Fig. 3.21 Characteristics of the outcrop of the sliding zone

Subsequent Reform of Landslide

The Huangtupo body with long-term slope deformation and sliding mass consists mainly of muddy stone blocks, and then it was subjected to reconstruction of tens of and even hundreds of thousands of years' weathering and denudation up until the present pattern.

On June 10, 1995, a landslide occurred on the top stratum of Erdaoqiao, with the landslide plane in the form of a sector in terms of longitudinal length of 100 m, maximum width of 90 m, thickness of 5–13 m, and volume of $6.7 \times 10^4 m^3$. The landslide body slid toward Erdaogou from the east side, NW of Erdaogou; the landslide occurs in the deposition of stone blocks composed of T_2b^3. The direct trigger of this landslide was loading of solid waste and life water in the rear edge. The landslide occurred on the edge of the east side of the Huangtupo landslide; it was not caused by movement of the Huangtupo landslide, but by local reconstruction (Fig. 3.22).

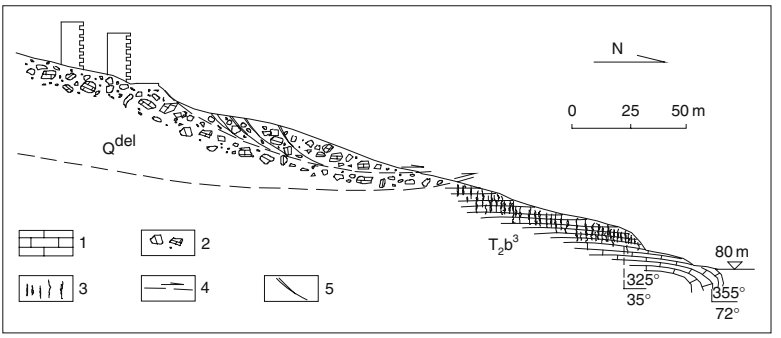

1. Pelmicrite; 2. Stone blocks deposition of landslide; 3. Cleavage; 4. Sliding plane; 5. Tension fissure

Fig. 3.22 Profile of Erdaogou landslides. 1 – Pelmicrite; 2 – stone blocks deposition of landslide; 3 – cleavage; 4 – sliding plane; 5 – tension fissure

On October 29, 1995, a landslide occurred in the west side of the Sidaogou outlet, which was in the form of a long sector with length of some 200 m, maximum width of around 100 m, and volume approximately of 20×10^4 m^3. The rear edge of the landslide had an elevation of some 150 m, sliding NE into the Yangtze River. The direct trigger of the landslide was rainfall and the fluctuation of water level of the Yangtze River. The landslide occurred in the stone block deposition of the Huangtupo landslide, identical to that of Erdaogou landslide in terms of an outcome of subsequent reconstruction of the Huangtupo landslide.

The occurrences of minor landslides in the Huangtupo area are reactivations of the ancient Huangtupo landslide. The stone blocks, forming the deposition of the Huangtupo landslide, are the physical preconditions contributing to the later, minor landslides due to their loose structure; in like manner, the river was flowing and washing, and gully washing produced steep landform, which led to powerful movement of landslides. Rainfall, fluctuation of water level of the Yangtze River, and possible earthquakes are direct triggers of landslides.

Landslide Evolution Pattern

According to conclusions provided through study of the formation and the evolution of the Huangtupo landslide, we can draw the chart of landslide evolution pattern, as shown in Fig. 3.23.

The 1st phase (a), slope development, river washes downward and causes formation of the Huangtupo slope;

The 2nd phase (b), deformation of the slope due to long-term action of gravity, the river washes out, in a continuous, downward motion , the front edge of the slope is hollowed, with toppling deformation in the shallow section. The surface rock mass disperses and rolls out along with the occurrence of loosely consolidated deposition; the shear strength concentration zone in the deep slope forms and develops and causes creep deformation;

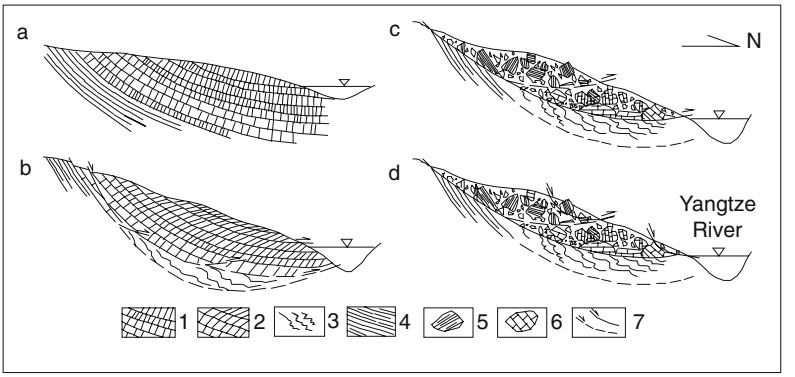

1. Cleaved muddy pelmicrite; 2. Toppled and deformed cleaved muddy pelmicrite; 3. Creep landslide zone; 4. Muddy siltstone; 5. Stone block deposition; 6. Landslide plane

Fig. 3.23 Slope deformation and landslide pattern of the Huangtupo landslide. 1 – Cleaved muddy pelmicrite; 2 – toppled and deformed cleaved muddy pelmicrite; 3 – creep landslide zone; 4 – muddy siltstone; 5 – stone block deposition; 6 – landslide plane

The 3rd phase (c), landslide phase, when the river washes out continuously downward, due to the long-term deformation which develops to certain extent, and some creep sliding deformation planes intersect and lead to a large-size landslide;

The 4th phase (d), reconstruction phase, when local reconstruction of the landslide occurs as a result of variation of external condition and on the basis of large-size landslide.

Conclusions

(1) The strata of the Badong formation are distributed widely in the Three Gorges reservoir area, where it tends to form large-size landslides and deep loosely consolidated geological body; hence it is a typical slide-prone stratum.

(2) The strata of the Badong formation in the Three Gorges reservoir area can be divided into five sections, and the lithology combinations are characterized by sandwich of soft and hard strata. Spatially, the lithology and lithological combinations are characterized by unique law of variation.

(3) The strata of the Badong formation are characterized by rich variation, an outcome of long-term slope deformation as well as all-important evidence for understanding the triggers and mechanism of landslide formation.

(4) The Huangtupo landslide is representative of the development of the Badong formation, along which the major deformation and destruction are important evidences in studying division of landslide development phases, landslide formation mechanism, landslide subsequent reconstruction, and landslide evolution pattern.

References

Carey SW (1953) The rheid concept in geotectonics. Geol. Soc. Aust. J., 1: 67–117

Fu ZR, Cai XL (1996) Tectonics of Epimetamorphic Rock Region. Geological Publishing House, Beijing, 21–32

Savage WZ, Varnes DJ (1987) Mechanics of gravitational spreading of steep-sided ridges ("Sackung"). Eng. Geol., 35: 31–36

Wu YF (1996) Huangtupo landslide and its geological background. In: Cui ZQ, Deng QL (eds.) Paper Collection on Geotechnical Engineering. China University of Geosciences Press, Wuhan, pp. 93–97

Zischinsky U (1966) On the deformation of high slopes. Proc. 1st Cong. Int. Soc. Rock Mech. 2: 179–185

Zong LX, Yin YP, Tang C (1996) Geological study on the new Badong County site in the Three Gorge Reservoir area planned to move. In Paper Collection of the Institute of Environment & Geology, Ministry of Geology and Mineral Resources. Geological Publishing House, Beijing, 1: 41–53